Japanese Journal of Applied Physics

RAPID COMMUNICATIONS

UV-laser-induced orientation of ZnO seed layer crystals for the growth of ZnO nanorods

To cite this article: Qiyan Zhang *et al* 2018 *Jpn. J. Appl. Phys.* **57** 070306

Japanese Journal of Applied Physics **57**, 070306 (2018) **RAPID COMMUNICATION**
https://doi.org/10.7567/JJAP.57.070306

UV-laser-induced orientation of ZnO seed layer crystals for the growth of ZnO nanorods

Qiyan Zhang, Mitsuhiro Honda, Shinji Takayanagi, and Yo Ichikawa

Graduate School of Engineering, Nagoya Institute of Technology, Nagoya 466-8555, Japan

*E-mail: cjv16504@stn.nitech.ac.jp

Received March 5, 2018; accepted April 26, 2018; published online June 13, 2018

We found that UV laser irradiation on a ZnO seed layer induced the crystal orientation at the surface, consequently leading to the growth of densely aligned ZnO nanorods on such a laser-irradiated layer. A single nanosecond pulse with a wavelength of 266 nm was irradiated to a ZnO seed layer on a glass substrate, and then, ZnO nanorods were synthesized on a laser-treated layer by a hydrothermal method. Electron microscopic observations revealed the growth of highly oriented ZnO nanorods on a laser-irradiated seed layer as well as the orientation of seed layer crystals to [0001]. © 2018 The Japan Society of Applied Physics

As a functional nanomaterial, ZnO nanorods are demonstrated to be applicable to many optoelectronic devices such as ultraviolet lasers[1,2] and active matrix liquid crystal displays.[3]

ZnO nanorods are generally grown on a seed layer, which is prepared preliminarily on a substrate utilizing several techniques.[4–10] The morphology of ZnO nanorods is known to be determined by the crystallinity of the seed layer. High temperature annealing (at 200–1000 °C) has been applied to improve the crystallinity of the seed layer,[11] on which well-aligned ZnO nanorods were shown to be grown.

We demonstrated the UV laser irradiation of ZnO seed layers for the growth of densely aligned ZnO nanorods. When a ZnO seed layer is irradiated by a UV laser, UV photons are well absorbed at the seed layer surface (depth of penetration into ZnO: 15–52 nm), and then, the crystals are rapidly heated and cooled for recrystallization. Compared with the conventional annealing method using furnaces or lamps, this method allows for a much less heating effect on a substrate as well as a rapid process in air. In this study, after the UV laser (266 nm wavelength) irradiation of a ZnO seed layer, both the laser-treated layer surface and the further grown ZnO nanorods were carefully studied by electron microscopy.

A ZnO seed layer was formed by RF magnetron sputtering.[12] We used glass (Corning EAGLE XG®) as a substrate, which is not applicable to high-temperature annealing ($\gtrsim$400 °C) owing to tremendous thermal expansion and deformation. A glass substrate was fixed in the chamber of an RF magnetron sputtering system located 50 mm away from a sintered ZnO target (99.99% purity, Kojundo Chemical Laboratory). The chamber was evacuated to a pressure of less than 1×10^{-4} Pa by a diffusion pump, and plasma was generated. The sputtering gases used were argon and oxygen, whose flow rates were adjusted to 2.8 and 0.7 sccm using a gas flow controller, respectively. After pre sputtering for 15 min, ZnO thin films were sputter-deposited at room temperature at a process pressure of 1 Pa with an RF power of 100 W. The thickness of seed layers was controlled from 150 to 400 nm by changing the deposition time.

A nanosecond pulsed Nd:YAG laser with a wavelength of 266 nm was applied to irradiate seed layers. The repetition rate was 10 Hz. A laser beam was focused on the seed layer surface, and scanning was performed to irradiate a single pulse on a seed layer. The focused beam diameter was 50 µm. To examine the effect of laser fluence, the laser power was changed from 1 to 9 mW, which correspond to 5.1 and 45.8 mJ/cm^2 per pulse on a focal plane, respectively. The laser-annealed seed layer surface was observed by scanning electron microscopy (SEM JEOL JSM-5600), and the crystal orientation of ZnO seed layers was measured by electron backscatter diffraction (EBSD).

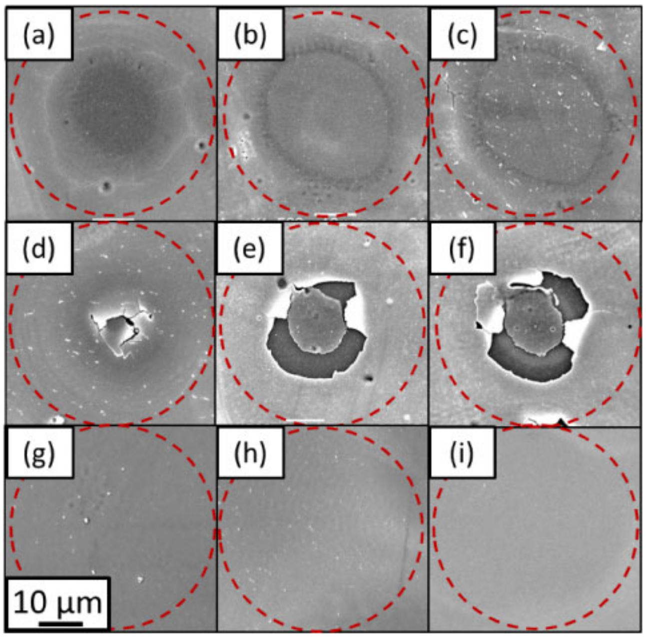

Fig. 1. (Color online) SEM images of UV-laser irradiated seed layers of 150 nm (a–c), 300 nm (d–f), and 400 nm (g–i) thicknesses. Panels (a, d, g), (b, e, h), and (c, f, i) correspond to different laser output powers of 1, 5, and 9 mW (5.1, 25.5, and 45.8 J/cm^2), respectively. The dotted circles with a red color denote the laser spot area.

On the laser-treated seed layers, ZnO nanorods were grown by hydrothermal synthesis following the procedure reported in Refs. 13 and 14. The surface morphology of ZnO nanorods was observed by SEM.

Figure 1 shows the SEM images of laser-treated seed layers with different thicknesses (150, 300, and 400 nm), where red circles show the area of laser focus. The laser powers applied are 1, 5, and 9 mW in panels (a, d, g), (b, e, h), and (c, f, i), respectively. From the dark contrast or the structural change at the surface in Figs. 1(a)–1(f), laser annealing is expected to be efficient for thin seed layers (150 and 300 nm thicknesses) but not for a 400-nm-thick layer, which shows no significant change in surface morphology. Noted that nanoscale grains are seen in Figs. 1(a)–1(c) at the center of the laser-irradiated area, which probably has a higher laser intensity. Taking

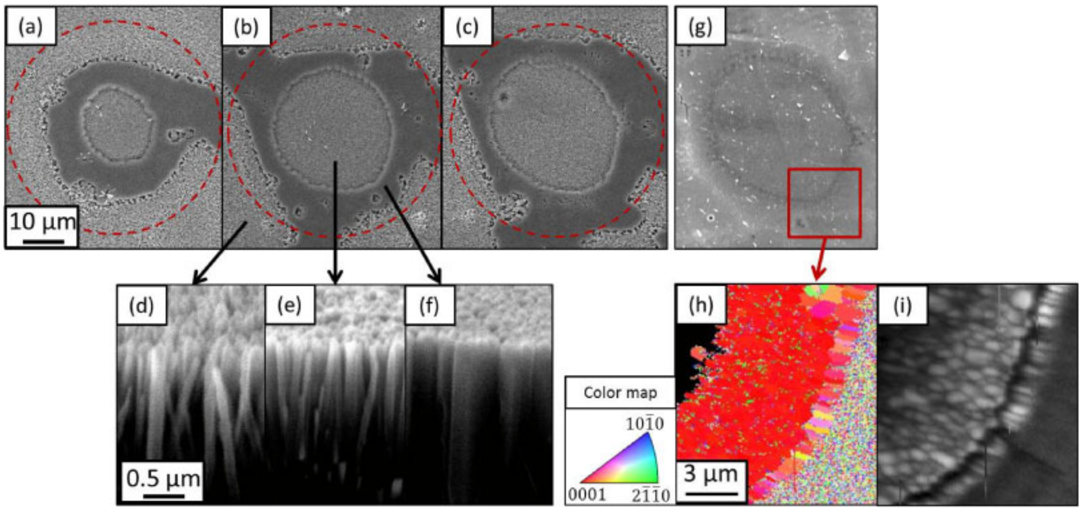

Fig. 2. (Color online) SEM images of ZnO nanorods grown on seed layers of 150 nm thickness irradiated by UV laser with different powers (a–f). Panels (a), (b), and (c) correspond to laser powers of 1, 5, and 9 mW, respectively. Panels (d), (e), and (f) show the enlarged cross-sectional views of panel (c). Panel (g) shows the SEM image of a 150-nm-thick seed layer irradiated by a UV laser at a laser power of 9 mW. Panels (h) and (i) show the IPF and IQ maps of a seed layer where a red rectangle is indicated in Fig. 2(g), respectively. Red, blue, and green colors in panel (h) indicate the crystal orientations of (0001), (10$\bar{1}$0), and (2$\bar{1}\bar{1}$0), respectively.

into account that the laser intensity used in our study was much higher than the ablation threshold (~0.45 J/cm^2),[15] the surface of a ZnO seed layer is expected to be ablated to possibly form a granular surface. Regarding the fact that seed layers of 300 nm thickness are seen to be partially peeled via laser irradiation, a thin seed layer (150 nm thick) is believed to be appropriate for efficient laser annealing while maintaining its continuous layer, a though its surface is slightly roughened by laser ablation.

Considering that the pulse width of a nanosecond laser is long enough to induce an instantaneous laser heating, the thermal energy given to the seed layer is expected to play a crucial role in laser annealing. Since the thermal conductivity of the EAGLE XG glass substrate is 1.29 W m^{-1} K^{-1}, which is less than that of ZnO (25.2 W m^{-1} K^{-1}), we expect that the heat generated at the 400-nm-thick seed layer surface will diffuse quickly enough to avoid the localization of thermal energy. The effect of thermal conductivity on laser heating was also supported by an additional test in which the 150 nm thin seed layer on a thermally conductive substrate (silicon) was laser-irradiated with 45.8 J/cm^2 laser intensity. In that experiment, any laser annealing or ablation was confirmed to be absent through surface observation by SEM measurements.

Figures 2(a)–2(c) show the SEM images of ZnO nanorods grown on 150-nm-thick seed layers irradiated by different laser powers, 5.1, 25.5, and 45.8 J/cm^2, respectively. Panels (d) and (e, f) are cross-sectional views of ZnO nanorods grown on unannealed and annealed layers, respectively. As shown in Figs. 2(e) and 2(f), two types of ZnO nanorods are found on a seed layer. Thin products are clearly seen in Fig. 2(e) to be distributed at the center of the irradiated area, while densely aligned ZnO nanorods are found at the surrounding area. The seed layer crystals at the area where dense products are seen are expected to be well crystallized, which leads to the improvement in orientation. Indeed, highly oriented and densely distributed ZnO nanorods have often been grown on highly crystallized seed layers by conventional thermal treatment.[16,17] On the other hand, as mentioned above, the surface of the laser-irradiated area tends to be ablated to be granular, resulting in such products with small diameters compared with those grown on unannealed layers.[18,19] To investigate the crystal structure of seed layers, EBSD measurement was conducted.

Figure 2(h) shows the inverse pole figure (IPF) map of a seed layer, where a red rectangle is indicated in Fig. 2(g). According to the IPF map, crystal planes with different orientations can be seen in the ZnO seed layer surface. The ZnO crystals at the outer edge of the laser-irradiated region are oriented in the [0001] direction, while those in the unannealed area are randomly oriented. The black area indicated in Fig. 2(h) corresponds to an unmeasurable area because of a very weak signal, which is consistent with the fact that a thin seed layer was generated by laser irradiation with an intensity much higher than the ablation threshold. The image quality (IQ) map of the same area in Fig. 2(g) is shown in Fig. 2(i), where a bright contrast shows a high crystallinity. The outer edge of the laser-irradiated region is considered to consist of highly crystallized ZnO particles. On the other hand, a low crystallinity was found at the center of the laser-irradiated area, which is expected owing to the laser ablation with high laser irradiation intensity.

From Fig. 2, the well-aligned ZnO nanorods are found to grow densely on the seed layer consisting of highly crystallized ZnO with an alignment in the [0001] direction. It is observed that the product tends to align even on the unannealed seed layer that exhibits a random crystal orientation. Since the ZnO crystal shows crystallographic polarity to [0001], nucleation is expected to occur dominantly on the (0001) plane, and consequently, ZnO nanorods were grown preferentially along the direction perpendicular to the substrate.

The improvement in nanorod alignment is also seen with 300-nm- and 400-nm-thick seed layers. Figures 3(a)–3(c) and 3(d)–3(f) show the SEM images of ZnO nanorods grown on laser-annealed seed layers of 300 and 400 nm thicknesses, respectively. With the 300-nm-thick seed layer, thick nanorods with improved orientation are seen at the center, those with poor orientation are observed in the ablated area. The slight improvement in nanorod orientation is seen even in

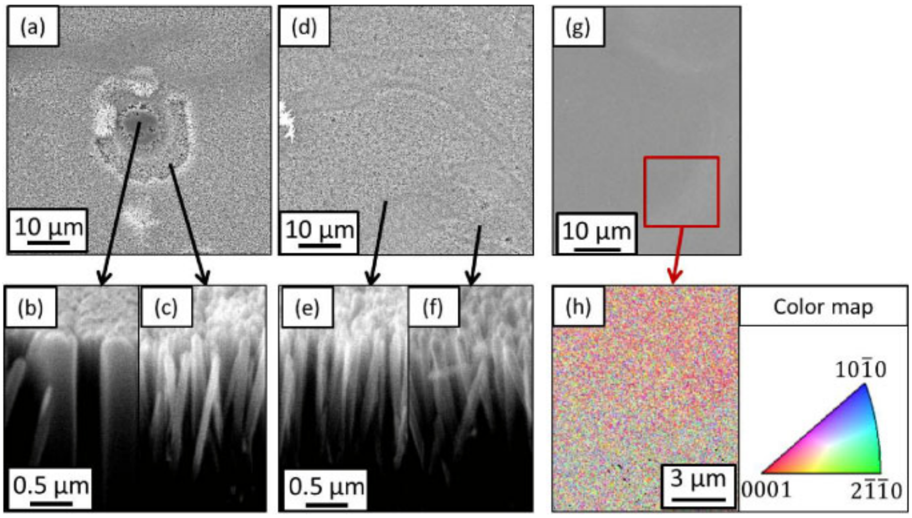

Fig. 3. (Color online) SEM images of ZnO nanorods grown on seed layers of 300 nm (a) and 400 nm (d) thicknesses irradiated by UV laser with 9 mW. Panels (b) and (c), and (e) and (f) show enlarged cross-sectional views of panels (a) and (b), respectively. Panel (g) shows the SEM image of a seed layer of 400 nm thickness irradiated by a UV laser with a laser power of 9 mW. Panel (h) shows the IPF map of the area indicated by a red rectangle in Fig. 3(g). Red, blue, and green colors in panel (h) indicate the crystal orientations of (0001), $(10\bar{1}0)$, and $(2\bar{1}\bar{1}0)$, respectively.

the laser-annealed area of 400 nm thickness, as shown in Figs. 3(d)–3(f). The EBSD observation result [Fig. 3(h)] of 400-nm-thick seed layer [Fig. 3(g)] explains that the moderate alignment of nanorods is attributed to the partially oriented crystals of ZnO seed layers. Thus, UV laser annealing is confirmed to be fast and efficient for aligning the ZnO crystals oriented to (0001) as well as for the growth of dense ZnO nanorods with improved orientation. In addition, we used a glass substrate considered unsuitable for developing a highly crystallized seed layer through thermal annealing (>400 °C), which implies that UV laser annealing is potentially applicable for a heat-sensitive substrate, although instantaneous laser heating is involved.

In conclusion, the UV laser annealing of ZnO seed layers on a glass substrate was demonstrated to grow densely aligned ZnO nanorods. By irradiating ZnO seed layers with a 266 nm pulsed laser, ZnO crystals at the seed layer surface were found to face the [0001] direction, which resulted in the growth of ZnO nanorods with improved orientation. The use of a thin seed layer or a substrate with low conductivity provided oriented crystals efficiently, suggesting the contribution of instantaneous heating due to ns pulses. The UV laser annealing technique demonstrated in this study is believed to be useful in controling the morphology of ZnO nanorods on various substrates being likely to be deteriorated at high temperatures, such as glass and ITO.

Acknowledgements This research was supported by JSPS KAKENHI Grant Number 17K05103. We thank Professor Masaki Tanemura for SEM measurement and Professor Tadachika Chiba for EBSD measurement.

1) M. Kawasaki, A. Ohtomoa, I. Ohkubob, H. Koinuma, Z. K. Tang, P. Yua, G. K. L. Wong, B. P. Zhang, and Y. Segawa, Mater. Sci. Eng. **56**, 239 (1998).
2) M. H. Huang, S. Mao, H. Ferick, H. Yan, Y. Wu, H. Knd, E. Weber, R. Russo, and P. Yang, Science **292**, 1897 (2001).
3) N. Yamamoto, H. Makino, S. Osone, A. Ujihara, T. Ito, H. Hokari, T. Maruyama, and T. Yamamoto, Thin Solid Films **520**, 4131 (2012).
4) C. H. Xu, H. F. Lui, and C. Surya, Mater. Lett. **65**, 27 (2011).
5) E. Fazio, A. M. Mezzasalma, G. Mondio, T. Serafino, F. Barreca, and F. Caridi, Appl. Surf. Sci. **257**, 2298 (2011).
6) N. K. Singh, S. Shrivastava, S. Rath, and S. Annapoorna, Appl. Surf. Sci. **257**, 1544 (2010).
7) M. Smirnov, C. Baban, and G. I. Rusu, Appl. Surf. Sci. **256**, 2405 (2010).
8) A. Sayari, A. Marzouki, A. Lusson, M. Oueslati, and V. Sallet, Thin Solid Films **518**, 6870 (2010).
9) S. Uthanna, T. K. Subramanyam, B. Srinivasulu Naidu, and G. Mohan Rao, Opt. Mater. **19**, 461 (2002).
10) M. Suchea, S. Christoulakis, N. Katsarakis, T. Kitsopoulus, and G. Kiriakidis, Thin Solid Films **515**, 6562 (2007).
11) V. Gupta and A. Mansingh, J. Appl. Phys. **80**, 1063 (1996).
12) X. C. Wang, X. M. Chen, and B. H. Yang, J. Alloys Compd. **488**, 232 (2009).
13) N. Uekawa, R. Yamashita, Y. Wu, and K. Kakegawa, Phys. Chem. Chem. Phys. **6**, 442 (2004).
14) L. Vayssieres, K. Keis, S. Lindquist, and A. Hagfeldt, Chem. Mater. **13**, 4395 (2001).
15) M. Jadraque, C. Domingo, and M. Martín, J. Appl. Phys. **104**, 024306 (2008).
16) A. Umar, B. Karunagaran, E.-K. Suh, and Y. B. Hahn, Nanotechnology **17**, 4072 (2006).
17) S. H. A. Yunus, M. Z. Sahdan, and S. A. Kamaruddin, ARPN J. Eng. Appl. Sci. **11**, 13247 (2016).
18) S. Pokai, P. Limnonthakul, M. Horprathum, P. Eiamchai, V. Pattantsetakul, S. Limwichean, N. Nuntawong, S. Porntheeraphat, and C. Chitichotpanya, Mater. Today **4**, 6336 (2017).
19) B. İkizler and S. M. Peker, Thin Solid Films **558**, 149 (2014).

